2010

Collinear phase matching for second harmonic generation using conoscopic interferometry

A Puri
University of New Orleans

A De

Recommended Citation

J. Appl. Phys. 107, 083104 (2010)

Collinear phase matching for second harmonic generation using conoscopic interferometry

A. De[1,2,a)] and A. Puri[1]
[1]Department of Physics, University of New Orleans, New Orleans, Louisiana 70148, USA
[2]Department of Physics, University of Wisconsin–Madison, Wisconsin 53706, USA

(Received 20 October 2009; accepted 2 February 2010; published online 26 April 2010)

The problem of finding phase-matching directions in noncentrosymmetric biaxial crystals is simplified here by the use of Conoscopic interferometry. Based on vector relations for wave propagation in birefringent media and solutions to phase-matching equations, we show that phase matching directions can be located on the conoscopic interferograms and that fringe numbers for dark-isochromes can be used as a guide to find phase-matching directions for a biaxial crystal. This technique can be generalized and extended to any anisotropic crystal. We have demonstrated this method for the particular case of a biaxial $KTiOPO_4$ crystal, where it is found to be particularly suitable for finding the optimum-phase-matching directions. *© 2010 American Institute of Physics*. [doi:10.1063/1.3354050]

I. INTRODUCTION

Second harmonic generation (SHG) continues to be one of the primary techniques for the generation of shorter wavelength laser light.[1,2] Since the first SHG experiment, performed by Franken *et al.*[3] in 1961, the conversion efficiency has been improved by utilizing higher power lasers, phase-matching (PM) techniques and superior nonlinear crystals, such as $KTiOPO_4$ (KTP),[4] $RbTiOPO_4$,[5] and their isomorphs from the titanyl arsenate family.[6] KTP-type crystals continue to be extremely popular for SHG as they are capable of both type-I and type-II PM over a wide range of temperatures. For both types of PM conditions, the fundamental beam has to be incident on the surface of the crystal at an optimal PM (OPM) angle.

In general, for any birefringent crystals, the PM conditions are obtained by varying the orientation of the crystal with respect to its optic-axis (for uniaxial crystals) or the acute/obtuse bisectrix (for biaxial crystals). It is well known that various crystallographic directions of high optical symmetry can be easily identified using Conoscopic interferometry. Conoscopic interferometric techniques have been used successfully to align surface-acoustic-wave substrate crystals,[7,8] identify crystal inhomogeneities,[9,10] determine refractive indices for nonlinear optical crystals,[11–15] to study phase transitions in birefringent liquid crystals and to determine their optical properties.[16–18] More recently a conoscopic technique was proposed for grinding and polishing plane optical surfaces normal to a uniaxial crystal's optic axis.[19]

In the case of uniaxial crystals, the existence of a single optic-axis allows symmetry of revolution, which simplifies the alignment process for finding PM directions. Conoscopic interferometric techniques have been successfully used to find PM directions in uniaxial KDP crystals.[20] However, it is much more difficult to find PM directions for biaxial crystals (such as KTP) due to its greater lack of optical symmetry.[21–23] Additional difficulties are encountered while trying to orient biaxial crystals to a desired PM direction due to their finite walk-off angles.[24]

In this article, we propose a technique to address this problem of finding PM directions for biaxial crystals by using simple vector analysis to project PM directions for the optically birefringent crystal onto its own conoscopic interferogram. As the fringes on a conoscopic interferogram are stable patterns of equiphase retardation, they can be used as a visual guide to find desired PM directions for any birefringent crystal. This is shown for the specific case of a KTP crystal, where we use dispersion dependent wave-propagation equations in crystalline media to obtain sets of fringe-numbers (when illuminated at $\lambda=633$ nm) and show that they correspond to particular PM directions (for a fundamental optical pump beam of $\lambda=1064$ nm). Projections of type-I and type-II PM directions are then charted with respect to the isochromes on a conoscopic interferogram for a KTP crystal. In general, this method can be used for finding the PM/OPM direction in any optically birefringent crystal. The description the PM loci generally adheres to the standardized frames recommended in Ref. 25. Very good agreement is seen between our calculated and experimentally observed conoscopic interferograms.

The general outline of this paper is as follows. In Sec. I, we briefly review the necessary conditions for achieving PM. This is followed by a description of the phase retardation patterns observed in conoscopic images for anisotropic crystals, in Sec. II. Experimental results, the crystal alignment procedures and the results of our calculations are discussed in Sec. III, followed by a brief summary.

II. BACKGROUND

It is well known that optically induced second harmonics are generated in crystalline media where inversion symmetry is lacking. The nonlinear response in the polarization of a crystalline medium to an intense laser beam causes the medium to develop new polarization frequency components,

a)Electronic mail: amritde@gmail.com.

which acts as the source of the frequency-doubled optical radiation. The degree of efficiency for production of the frequency-doubled radiation is given by the well known expression,[26,27]

$$\eta = \frac{P_3}{P_1} = C d_{\text{eff}}^2 I_f L^2 \frac{\sin(\delta k L/2)}{\delta k L/2}, \quad (1)$$

where P_3 denotes power of the frequency-doubled radiation, P_1 is the power of the fundamental wave, C is a constant, d_{eff} is the effective-nonlinear-coefficient, I_f is the intensity of the fundamental wave with regard to the beam cross-section, L is the length of the crystal, and k is the wave-number. For SHG, as $\omega_1 = \omega_2 = \omega_3/2$, one gets $\delta k = k_3 - 2k_1$. It is not possible to satisfy this condition in an optically isotropic crystal due to its normal dispersion relations and hence requires the use of a birefringent crystal. In a birefringent crystal, the phase-velocities of the interacting beams can be adjusted to satisfy PM conditions for their respective wave-vectors. The degree of birefringence is highest for optically biaxial crystals as no two crystallographic directions are equivalent. Subsequently for any given direction of ray propagation, there exist three different principle indices of refraction. The relation between ray propagation and ray velocity directions can be determined by using Maxwell's equations. The Fresnel's equation for plane wave propagation in a birefringent media is given by,[26]

$$\frac{k_x^2}{n^2 - n_x^2} + \frac{k_y^2}{n^2 - n_y^2} + \frac{k_z^2}{n^2 - n_z^2} = \frac{1}{n^2}, \quad (2)$$

where, $k_x = \sin(\theta)\cos(\phi), k_y = \sin(\theta)\sin(\phi), k_z = \cos(\theta)$ are components of the unit wave-vector, n_j are principal crystal refractive indices for a given wavelength and n is the refractive index in a given direction.

By solving for n in Eq. (2) one obtains two orthogonally-polarized normal modes of propagation, $n'(\phi,\theta)$ and $n''(\phi,\theta)$. These are, respectively, referred to as the ordinary and extraordinary refractive indices. In the direction of the optic axis $n' = n''$, subsequently, this yields the following expression for the angle between the optic-axes and the z-axis (acute-bisectrix) for an optically biaxial crystal[26]

$$\tan(\beta) = \frac{k_x}{s_z} = \frac{n_z}{n_y}\sqrt{\frac{n_y^2 - n_x^2}{n_z^2 - n_y^2}}, \quad (3)$$

The phase difference between the ordinary and extraordinary modes of propagation, for an optically biaxial-crystal, is given by,

$$\delta = \frac{\pi h (n_z - n_y)}{\lambda \cos(\psi_2)} \sin^2(\psi_1)\sin^2(\psi_2), \quad (4)$$

where, λ is the optical-wavelength, h is the crystal-thickness. ψ_1 and ψ_2 are the angles the wave-normal, $\vec{\mathbf{k}}$, makes with the two optic-axis, O_1 and O_2, respectively, and is expressed as $\cos(\psi_1) = k_x \sin(\beta) + k_z \cos(\beta)$ and $\cos(\psi_2) = -k_x \sin(\beta) + k_z \cos(\beta)$. The Bertin's surfaces of constant phase difference between ordinary and extraordinary waves for an optically biaxial crystal are shown in Fig. 1.

There are several ways to achieve PM for birefringent crystals. Among them angle-tuning is the most common method, which can be further classified into type-I and type-II PM. Type-I PM corresponds to the two fundamental beams having the same polarization, whereas type-II PM corresponds to the two beams being orthogonally polarized. For a positive biaxial crystals, such as KTP, type-I PM directions are obtained by solving,[28]

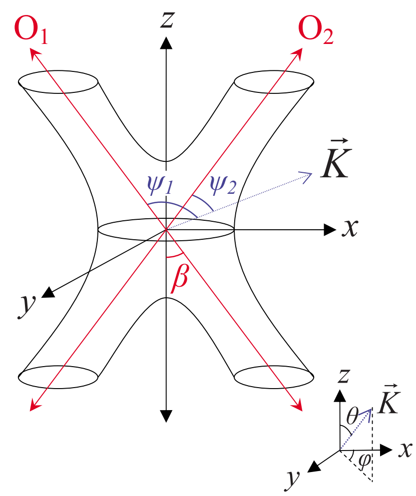

FIG. 1. (Color online) Bertin surfaces of constant phase difference between ordinary and extraordinary rays for an optically biaxial crystal.

$$B_\omega(1 + \zeta_\omega) = B_{2\omega}(1 - \zeta_{2\omega}), \quad (5)$$

For type-II PM, the following approximate expression can be solved to find PM directions,[28]

$$B_\omega(1 + \zeta_\omega^2/2) = B_{2\omega}(1 - \zeta_{2\omega}/2)^2, \quad (6)$$

where,

$$B_i = \frac{1 - k_z^2}{n_{z,i}^2} + \frac{k_z^2 + k_y^2}{n_{x,i}^2} + \frac{k_z^2 + k_x^2}{n_{y,i}^2}, \quad (7)$$

$$C_i = \frac{k_z^2}{n_{x,i}^2 n_{y,i}^2} + \frac{k_y^2}{n_{x,i}^2 n_{z,i}^2} + \frac{k_x^2}{n_{y,i}^2 n_{z,i}^2}, \quad (8)$$

$$\zeta_i = \sqrt{1 - 4C_i/B_i^2}, \quad (9)$$

The index i, takes on ω, for the fundamental frequency and 2ω, for the second-harmonic.

Among various PM directions, there exists an OPM, which is determined by the effective nonlinear coefficient. For the particular case of a KTP crystal, the calculated OPM direction is at $\theta = 90°$ and $\phi = 21.5°$,[28] for a fundamental beam with $\lambda = 1064$ nm. These calculated values are in very good agreement with experimentally measured OPM direction for KTP.

III. METHODOLOGY

In Sec. III, we discuss the use of conoscopic-interferometry for finding various PM directions for biaxial crystals. In particular, we demonstrate this for the case of a KTP crystal.

A conoscopic interferogram can be observed by using an optical setup, such as that shown in Fig. 2. The KTP crystal is mounted on a goniometer and placed between two crossed

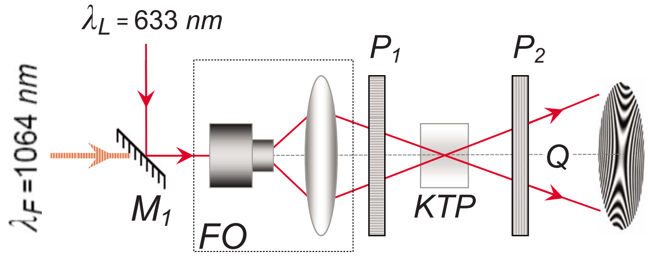

FIG. 2. (Color online) Optical setup for conoscopic interferometry and SHG generation. M1, P1, P2, and FO are, respectively, a mirror, polarizer, analyzer, and the focusing-optics. Orientation of P2 is orthogonal to P1. Q is the axis of the conoscopic-interferometer. λ_L and λ_F are the conoscopic-illumination-wavelength and the fundamental-pump-wavelength, respectively. The two laser-beams should be collinear. M1, P1, P2, and FO should be mounted on a foldable-mirror mount.

polarizers and illuminated using a diverging He–Ne laser beam. The intensity distribution pattern varies as a function of the angle-of-incidence. This results in the Conoscopic interference fringes as shown in Fig. 3, for the case of an x-cut KTP crystal. These fringes are stable patterns of isochromes or bands of equiphase retardation and can be calculated using Eq. (4), as shown in Figs. 4 and 5. The agreement between the calculated and observed conoscopic interferogram is excellent, as shown in the figures. Light rays that pass through the optic-axes, experience zero retardation, and form melatopes, as shown in Figs. 4 and 5. From the melatopes, phase retardation increases in all directions till it reaches its maximum along the optic-normal. In case of an x-cut KTP crystal, the melatopes are hard to observe as the angle between the optic-axis and the obtuse-bisectrix (x-axis) is $\approx 72°$ (when illuminated at $\lambda = 633$ nm).

Next, in order to demonstrate the application of the conoscopic interferometry for finding SHG PM directions, we calculated type-I and type-II PM directions (for a fundamental-frequency of 1064 nm), from Eqs. (5) and (6), respectively. These PM directions, ϕ_{PM} and θ_{PM}, are normalized to the calculated conoscopic interferogram and are then projected on to the $y-z$ plane, in the case of an x-cut crystal (Fig. 4) and $y-x$ plane, for a z-cut crystal (Fig. 5). Our calculated results for PM directions are identical to those obtained by Yao *et al.*[28] In the case of Fig. 4, both type-I and type-II PM directions are shown in Fig. 4, as they these directions are more easily accessible for a x-cut KTP crystal. Whereas in the case of a z-cut crystal, type-II PM directions would require very large polar-angle rotations hence only type-I PM solutions are projected onto the calculated conoscopic interferogram in Fig. 5.

As seen in Figs. 4 and 5, the PM directions intersect various isochromes. Therefore, it can be concluded that for a given azimuthal orientation, PM-type and a set of crystal parameters, there exists a unique fringe-number on the conoscopic interferogram which corresponds to a particular PM direction. Hence, we propose using the fringe-numbers for the dark-isochromes, as a visual guide to find PM directions in nonlinear-biaxial-crystals. For any given set of crystal parameters, the nearest dark fringe-number in the vicinity of a PM direction can be calculated as follows. The intensity distribution of the conoscopic interferogram is $\propto \cos^2(\delta)$, where δ is given by Eq. (4). In the case of a z-cut crystal, for any PM direction, δ_{PM} can be obtained by substituting the solutions ϕ_{PM} and θ_{PM} in Eq. (4). In the case of a x-cut crystal, one has to make the alternate substitution $\theta'_{PM} = \phi_{PM}$ and $\phi'_{PM} = \cos^{-1}[\cos(\theta_{PM})/\sin(\theta'_{PM})]$ (in place of θ_{PM} and ϕ_{PM}) in Eq. (4). This vector transformation is necessary since the PM solutions have to be projected on to the $y-z$ plane, for an x-cut crystal. Subsequently, the fringe-number for a dark-isochrome in the nearest vicinity of a PM direction can be obtained by equating $\delta_{PM} = (2m+1)\pi/2$ and solving for m.

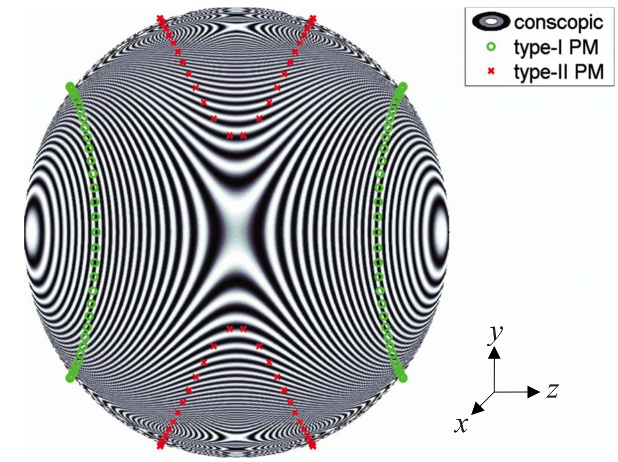

FIG. 4. (Color online) Calculated conoscopic interferogram for a x-cut KTP, for a illumination wavelength, $\lambda = 633$ nm. Corresponding projections for type-I and type-II PM on the $z-y$ plane, are shown. PM directions are calculated for a fundamental wavelength of 1064 nm. A thickness, $h = 0.5$ mm was chosen for the purpose of illustration.

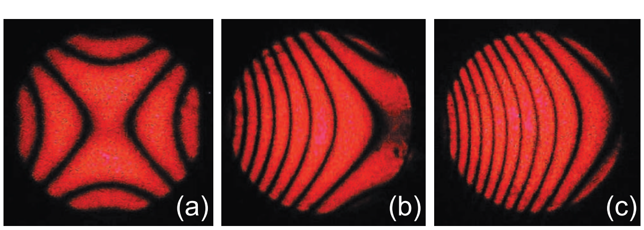

FIG. 3. (Color) Observed conoscopic interferograms for x-cut KTP at goinometer-rotation-angles of (a) 0°, (b) 5°, and (c) 10°.

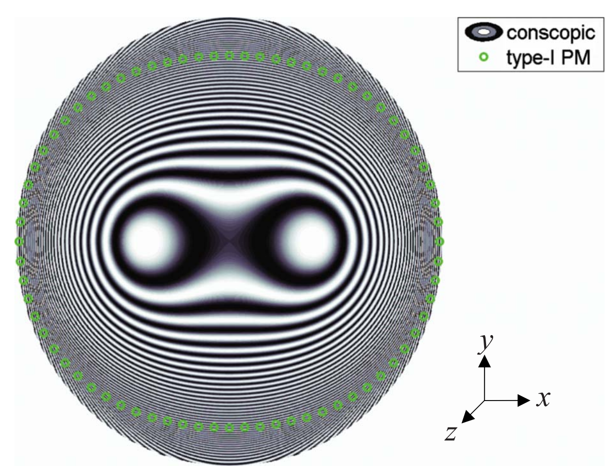

FIG. 5. (Color online) Calculated conoscopic-interferogram for a z-cut KTP, for a illumination wavelength, $\lambda = 633$ nm. Corresponding projections for type-I PM on the $x-y$ plane, are shown. PM directions are calculated for a fundamental wavelength of 1064 nm. A thickness, $h = 0.5$ mm was chosen for the purpose of illustration.

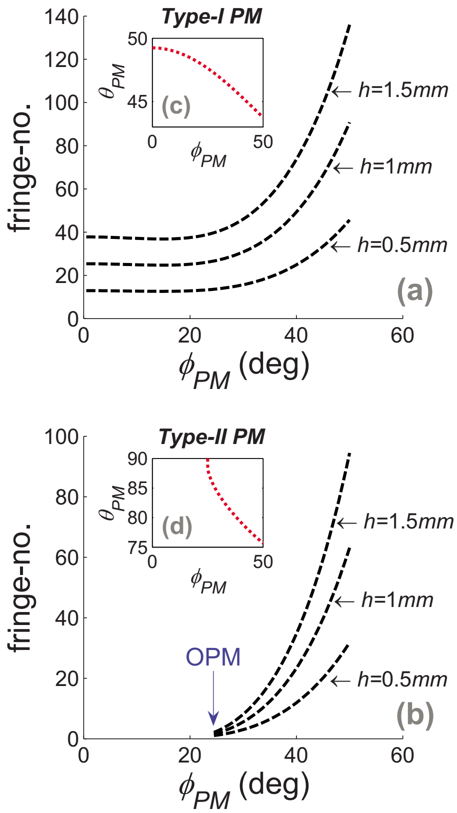

FIG. 6. (Color online) Calculated fringe-numbers showing the intersection of dark-fringes on the conoscopic interferogram to various PM directions for an x-cut KTP. The interferogram is calculated for an illuminating wavelength of 633 nm and the PM directions correspond to a fundamental-wavelength of 1064 nm. (a) Fringe-number corresponding to type-I PM directions, for various crystal thicknesses. (b) Fringe-numbers corresponding to type-II PM directions, for various crystal thicknesses. (c) Type-I PM. (d) Type-II PM.

These PM-fringe-numbers are shown in Fig. 6, for type-I and type-II PM in an x-cut KTP, as a function of ϕ_{PM} and for various crystal-thicknesses. Similarly in Fig. 7, PM-fringe-numbers are shown, for type-I directions in an z-cut KTP. As seen in Fig. 6, this technique can be particularly useful for finding the OPM ($\phi_{\text{OPM}}=21.5°$ and $\theta_{OPM}=90°$) direction in an x-cut KTP crystal. The OPM-fringe-numbers are shown in Fig. 6(a) and correspond to the intersection of the y-axis (since $\theta_{\text{OPM}}=90°$) and the projected type-II PM solutions in Fig. 4. The OPM-fringe-number=3, for a KTP crystal-thickness, $h=0.5$ mm. Interestingly, it is seen from our calculations that for every 0.5 mm increase in KTP crystal-thickness, the OPM-fringe-number increases by one. Note that these results correspond to an illuminating $\lambda=633$ nm and a fundamental pump-frequency of 1064 nm. In Fig. 6(a), it is seen that for x-cut crystals, lower ϕ_{PM} correspond to lower PM-fringe-numbers. Whereas in the case if an z-cut crystal, Fig. 7, higher ϕ_{PM} correspond to lower PM-fringe-numbers.

Once the conoscopic image is visible, the crystal can be rotated so that the PM-fringe-number is centered on the conoscopic interferogram. For example, to find the type-I principle PM-direction corresponding to $\phi_{\text{PM}}=0°$ and $\theta_{\text{PM}}=49.2°$, the KTP crystal should be rotated as shown in Fig. 3. It should be ensured that the $x-z$ plane is the plane of rotation for the crystal. This is easily done if the melatopes are visible, however, they are not easily observable in the case of x-cut KTP. In their absence the following alternative can be used. The $x-z$ plane can be identified by carefully observing the central isochromes along the direction of the obtuse-bisectrix. Unlike the case of uniaxial crystals in planar alignment, the central isochromes for biaxial crystals are nonsymmetric about the bisectrix. For a positive biaxial crystal, such as KTP, it is seen that the distance between the innermost fringes (or the central-isochromes) in the plane of the melatopes ($x-z$ plane) are the nearest. Therefore, the crystal should be azimuthally rotated so that the shortest distance between the central isochromes lie in the plane of rotation of the crystal. Rotations in the $x-z$ plane for this particular example is shown in Fig. 3. Note, that once the optic-normal (which is the obtuse (acute)-bisectrix in case of an $x(z)$-cut KTP) is centered in the interferogram, one can also rely on the goniometer's angle readout to rotate the crystal by a PM-angle. This, however, requires that rotation-axis passes through the crystal, to minimize alignment errors. One particular advantage of using fringe-numbers to find PM directions instead, is that it allows the crystal-position to be independent of the rotation-axis.

We propose the following simple setup to for alligning the KTP crystal, as shown in Fig. 2. The KTP crystal is inserted between two cross polarisers, preferably inserted in foldable mounts. The pump-laser-beam used for SHG and the illuminating-laser-beam used for conoscopy must be collinear. Once the conoscopic image is visible on the screen and the crystal has been rotated, such that the PM-fringe-number is centered, the pump-beam can be introduced using the foldable-mirror-mount.

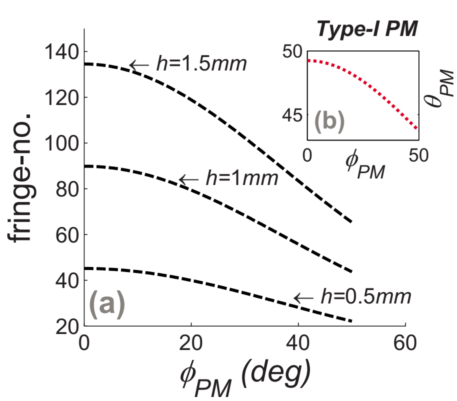

FIG. 7. (Color online) Calculated fringe-numbers showing the intersection of dark-fringes on the conoscopic interferogram to Type-I PM directions for an z-cut KTP. The interferogram is calculated for an illuminating wavelength of 633 nm and the PM directions correspond to a fundamental-wavelength of 1064 nm. (a) Fringe-number corresponding to type-I PM directions, for various crystal thicknesses. (b) Type-I PM.

IV. SUMMARY

In summary, we have shown that with the use of conoscopic interferometry and simple PM equations, the problem of finding optimum PM directions for biaxial crystals can be greatly simplified. Instead of blindly scanning a large number of polar and azimuthal angles, our proposed method allows one to find PM directions visually. This alignment technique based on solutions to a set of wave-propagation and PM equations. The use of conoscopic interferometry allows quick identification of the direction and orientation of the crystallographic-optic-axes and its acute/obtuse bisectrix. Thereafter, the fringe-number corresponding to a particular PM direction can be calculated and easily identified on the interferogram. This alignment technique is demonstrated here for the difficult case of a biaxial KTP crystal with nonvisible melatopes. In general, this technique simplifies the PM alignment procedure by providing a systematic visual guide and can be extended to any anisotropic nonlinear frequency doubling crystal. Our proposed fringe counting method could be used along with a charge-coupled-device to set up a calibrated system with feedback loops to automatically find optimal PM directions in optically uniaxial and biaxial crystals.

[1]S. Spiekermann, H. Karlsson, and F. Laurell, Appl. Opt. **40**, 1979 (2001).
[2]F. Hanson, Opt. Lett. **20**, 148 (1995).
[3]P. A. Franken, A. E. Hill, C. W. Peters, and G. Weinreich, Phys. Rev. Lett. **7**, 118 (1961).
[4]M. N. Satyanarayan, A. Deepthy, and H. L. Bhat, Crit. Rev. Solid State Mater. Sci. **24**, 103 (1999).
[5]C. A. Ebbers and S. P. Velsko, Appl. Phys. Lett. **67**, 593 (1995).
[6]A. H. Kung, Appl. Phys. Lett. **65**, 1082 (1994).
[7]P. Äyräs, A. T. Friberg, M. Kaivola, and M. M. Salomaa, J. Appl. Phys. **82**, 4039 (1997).
[8]P. Äyräs, A. T. Friberg, M. Kaviola, and M. M. Salomma, Appl. Opt. **38**, 5399 (1999).
[9]A. L. Bajor, L. Salbut, A. Szwedowski, and T. Piatkowski, Rev. Sci. Instrum. **69**, 1476 (1998).
[10]L. Dumitrascu, I. Dumitrascu, and D. O. Dorohoi, J. Appl. Crystallogr. **42**, 878 (2009).
[11]L. Isaenko, A. Yelisseyev, S. Lobanov, V. Petrov, F. Rotermund, G. Slekys, and J. J. Zondy, J. Appl. Phys. **91**, 9475 (2002).
[12]M. A. Geday and A. M. Glazer, J. Appl. Crystallogr. **35**, 185 (2002).
[13]Ch. Y. Gao, H. R. Xia, J. Q. Xu, Sh. Ch. Si, H. J. Zhang, J. Y. Wang, and H. L. Song, Cryst. Res. Technol. **42**, 1126 (2007).
[14]E. Gorecka, A. D. L. Chandani, Y. Ouchi, H. Takezoe, and A. Fukuda, Jpn. J. Appl. Phys. **29**, 131 (1990).
[15]A. Roy and N. V. Madhusudana, Europhys. Lett. **36**, 221 (1996).
[16]B. L. Van Horn and H. H. Winter, Appl. Opt. **40**, 2089 (2001).
[17]V. Manjuladevi and J. Vij, Liq. Cryst. **34**, 963 (2007).
[18]J.-K. Song, J. K. Vij, and B. K. Sadashiva, J. Opt. Soc. Am. A Opt. Image Sci. Vis. **25**, 1820 (2008).
[19]S. Chatterjee and Y. Pavan Kumar, Appl. Opt. **46**, 1435 (2007).
[20]M. J. Guardalben, Appl. Opt. **36**, 9107 (1997).
[21]L. T. Cheng, L. K. Cheng, J. D. Bierlein, and F. C. Zumsteg, Appl. Phys. Lett. **63**, 2618 (1993).
[22]W. Seelert, P. Kortz, D. Rytz, B. Zysset, D. Egglehausen, and G. Mizell, Opt. Lett. **17**, 1432 (1992).
[23]G. E. James, E. M. Harrell, C. Bracikowski, K. Weisenfeld, and R. Roy, Opt. Lett. **15**, 1141 (1990).
[24]L. K. Cheng, L. T. Cheng, and J. D. Bierlein, Appl. Phys. Lett. **64**, 1321, (1994).
[25]D. A. Roberts, IEEE J. Quantum Electron. **28**, 2057 (1992).
[26]A. Yariv and P. Yeh, *Optical Waves in Crystals* (Wiley, New York, 1984).
[27]T. Y. Fan, C. E. Huang, R. C. Eckardt, Y. X. Fan, R. L. Byer, and R. S. Feigelson, Appl. Opt. **26**, 2390 (1987).
[28]J. Q. Yao and T. F. Fahlen, J. Appl. Phys. **55**, 65 (1984).